Journal of Bio- and Tribo-Corrosion (2020) 6:125
https://doi.org/10.1007/s40735-020-00418-y

The Reactivity of the Corrosion Mechanism in Transformers: A Computational Study

Sharlene-Asia Naicker[1] · **Mervlyn Moodley**[1]

Received: 14 June 2020 / Revised: 28 July 2020 / Accepted: 20 August 2020 / Published online: 17 September 2020

Abstract
Density functional theory (DFT) and Monte Carlo (MC) techniques were used to investigate the adsorption behaviour of sulphur-containing molecules namely dibenzyl disulphide (DBDS) and copper sulphide (Cu_2S) on different copper (Cu) surfaces. These sulphides are involved in the corrosion of copper windings in power transformers. The structural and quantum chemical parameters such as the molecular orbital energies, energy gaps and chemical hardness of these sulphides were investigated along with its electronic and energetic properties. To allow successful adsorption, the initial lattice parameters were determined prior to geometry optimization of all molecules and surfaces. The lowest adsorption energy configurations with its corresponding adsorption and deformation energies were determined. The density of adsorption sites were also determined. An adsorption energy comparison was done between the DBDS and Cu_2S to determine the most reactive species on the different Cu surfaces. The reactivity of the two sulphides were investigated to provide a better understanding of the corrosion mechanism in transformers. The average bond distance between the sulphur (S) atom and the nearest Cu surface atom for the lowest energy configurations for both DBDS and Cu_2S were compared in order to understand the behaviour of the sulphides.

Keywords Copper corrosion · Transformer corrosion · Dibenzyl disulphide · Density functional theory · Adsorption locator · Monte Carlo

1 Introduction

The efficient running of power transformers is of worldwide concern after a significant number of transformers were found to be failing without warning [1]. These failures have put increased stress on the financial, social and economic sectors of the power industry. Transformer failures have been attributed to corrosive sulphur that has been found to react with the Cu surfaces [1–3]. One species of corrosive sulphur has been identified as dibenzyl disulphide (DBDS). The product of the reaction of DBDS ($(C_6H_5CH_2)_2S_2$) with a Cu surface results in Cu_2S as a first mechanism, given by Eq. 1, which reacts further with the Cu surface leading to the ultimate failure as a second mechanism.

$$4Cu\,(s) + (C_6H_5CH_2)_2S_2 \rightarrow 2Cu_2S(s) + C_6H_5CH_2CH_2C_6H_5. \quad (1)$$

There are several factors that influence the corrosion of transformers but they have also been identified to increase the reactivity of the DBDS. These factors include the temperature and electric field of the transformer, the type of oil and oxygen content and the concentration of DBDS in the transformer oil [2–8]. Research has also focused on applying first principle techniques to transformers but from a Dissolved Gas Analysis (DGA) perspective [9–11]. Research on DBDS and Cu_2S has mainly focused on laboratory studies while very few computational studies have been performed [2–7]. By determining the most influential sulphide in the mechanism brings us one step closer to understanding the formation mechanism of corrosion on cu surfaces.

S and Cu interactions have been studied extensively during the past years. The motivation for these studies have been due to the complexity of the S–Cu system [12–17]. The Cu bulk molecule can be divided into different crystalline

✉ Sharlene-Asia Naicker
sharlenenaicker@gmail.com

Mervlyn Moodley
moodleym2@ukzn.ac.za

[1] School of Chemistry and Physics, University of KwaZulu-Natal, Private Bag X54001, Durban 4000, South Africa

surfaces/planes namely: Cu(100), Cu(101) , Cu(110) and Cu(111) [13]. The surfaces themselves have different sites where sulphur atoms would likely attach [13]. As described in references [14, 17–19] a small amount of sulphur on the surface creates a distortion and vacancies in the copper.

Most research [12–17] has focused on the study of different atoms such as Pd, Ag, Cu and S on surfaces however a comparative study has not been done on DBDS and Cu_2S interacting with the different surface planes. DBDS and Cu_2S are categorized as thoils since they contain sulphur molecules [20]. Analyzing these thiols provide information about key properties known as quantum chemical parameters which include the energy gap, chemical hardness, softness and electronegetivity of the molecules [21–23].

In this paper we focus on determining the most reactive sulphur compound in the corrosion mechanism between the DBDS and the Cu_2S. Density functional theory (DFT) and Monte Carlo (MC) methods are commonly used to model interactions of atoms with surfaces and provides more information about the reactivity. Previous research on DBDS has focused primarily on determining the interaction using DFT [7], however our research focuses on employing both DFT and MC techniques in determining the density of sites of adsorption along with the bond length from the sulphur component to the Cu surface.

2 Computational Methods

Density functional theory (DFT) and Monte Carlo (MC) techniques from the Accerlys Materials Studio 2018 software were used to compute the adsorption of sulphides on Cu(100), Cu(101), Cu(110) and Cu(111) surfaces [24]. DFT is commonly used for determining the energies of periodic systems [7, 24]. The theory uses the electron density to determine the most stable structure with its ground state energy [21, 24, 25]. DFT has brought us closer to solving the problem of simulating large systems of molecules. It is a useful tool for understanding the electronic and energetic properties of systems and reduces the cost of computational time [7]. MC techniques have become very helpful in determining the lowest energy configurations and adsorption sites for different structures and surfaces [21, 26, 27].

The most efficient geometry optimization modules from the Materials Studio software were identified as the $Dmol^3$ package and Cambridge Sequential Total Energy Package (CASTEP) which were used throughout this computational study [24, 28, 29]. CASTEP is a significant DFT module that uses the plane wave generalized gradient approximations (GGA) to determine different parameters of structures, molecules and surfaces [29]. The $Dmol^3$ technique also uses DFT to determine the energy of molecules and

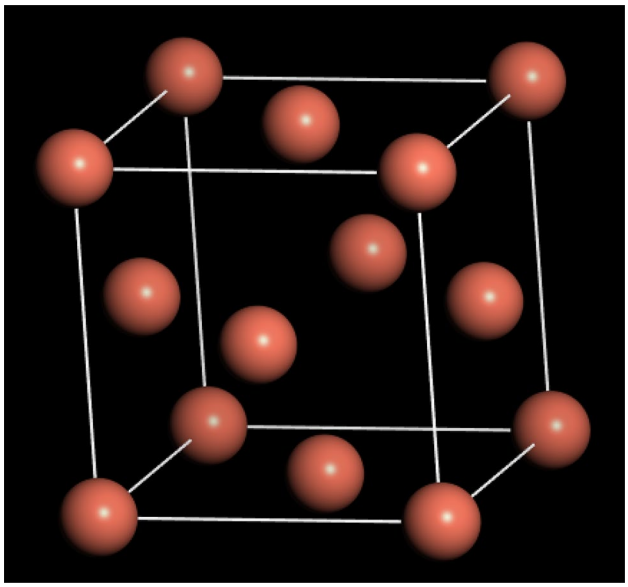

Fig. 1 Cu Bulk which contains 14 Cu atoms in a FCC structure

performs optimization without having to convert to a 3D periodic structure. Geometry optimization allows for an optimal atomic arrangment by rotating and translating the lattice parameter to create stable structure forms with minimal energy [24, 28, 30]. In this study, all bulk Cu surfaces and sulphide molecules were geometrically optimized using DFT techniques to create stable structures for the interactions to occur. The Cu bulk shown in Fig. 1 was optimized using CASTEP by determining the most suitable exchange-correlation functional, cutoff energy and k-point sampling. This was achieved by obtaining a lattice constant closest to the experimental value of 3.615 Å [16, 31]. The Cu bulk contains 14 Cu atoms with a face centered cubic structure which was cleaved into Cu surfaces namely Cu(100) , Cu(101), Cu(110) and Cu(111). The Cu surfaces were thereafter converted to a (3 × 3) supercell for adequate coverage for interactions to occur and a vacuum thickness of 10 Å, optimized using the CASTEP module [29]. The simulation method uses the vacuum slab model to create a 3D periodic structure. Figure 2 shows the Cu(110) surface as a (3 × 3) supercell slab model.

The DBDS and Cu_2S were also geometrically optimized using the $Dmol^3$ module before being adsorbed onto the Cu surfaces. The optimization is needed to create a stable adsorbate which interacts readily with the surface. Quantum chemical parameters/descriptors such as the energy of highest occupied molecular orbital ($E_{HOMO)}$and the energy of the lowest unoccupied molecular orbital ($E_{LUMO)}$ were also obtained from geometrically optimizing the DBDS and Cu_2S. The ($E_{HOMO)}$ is a measure of the ability of the

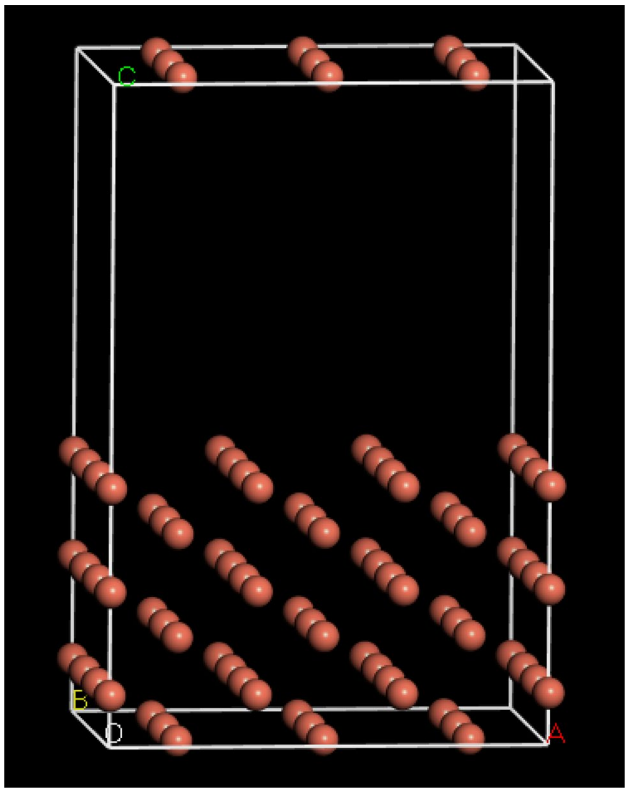

Fig. 2 A 3 × 3 supercell Cu(110) surface slab model

molecule to donate electrons [21–23]. Other quantum chemical parameters/ descriptors as explained in depth by references [22, 23, 32], are now defined below.

The energy gap for the molecular orbitals describes the binding ability of the molecule and is given by

$$\Delta E_{gap} = E_{HOMO} - E_{LUMO}. \quad (2)$$

The ionization potential (I) and electron affinity (A) are given as

$$I = -E_{HOMO} \quad (3)$$

and

$$A = -E_{LUMO}. \quad (4)$$

The electronegativity (χ), chemical hardness (η) and softness (δ) are calculated as

$$\eta = \frac{-E_{HOMO} + E_{LUMO}}{2}, \quad (5)$$

$$\delta = \frac{1}{\eta} \quad (6)$$

and

$$\chi = \frac{-E_{HOMO} - E_{LUMO}}{2}. \quad (7)$$

The adsorption energy was found using the MC techniques. The adsorption locator module in the Materials Studio software best represents the MC techniques and determines the lowest energy of the interaction of molecules on surfaces as shown in different references [21–24, 26, 27, 32, 33]. Through trial and error methods the Condensed-Phase Optimized Molecular Potentials for Atomistic Simulation (Compass) II Forcefield was found to be the most efficient to be used for simulations [24, 34]. This agrees with other work done, since this forcefield is commonly used in understanding a range of different interactions [21, 26]. The top layer of the different surfaces were allowed to relax prior to adsorption. The optimised DBDS and Cu_2S were randomly arranged on the different Cu surfaces by employing the Metropolis MC method which uses different criteria to obtain accurate adsorption sites and energies [21, 33]. The Adsorption Locator module provides information about the adsorption energy, the rigid adsorption energy and the deformation energy. The adsorption energy is the combination of the rigid adsorption energy and the deformation energy. The rigid adsorption energy is the energy released into the system and shows the energy prior to any changes on the surface. The deformation energy is the energy released when the surface undergoes a change and a portion of the adsorbate is removed to assist with the surface change. The initial substrate was set to zero similarly to the premise behind the research in references [21, 26, 33]. The density of adsorption illustrations also provide information on the sites where the adsorbate is most likely to interact. In this paper, these sites are referred to as Hollow or Top sites [7, 26]. The Top sites indicate the adsorbate interacting directly on top of the surface while the Hollow sites interact within the surface [7, 26]. The shortest bond lengths between the S atoms from the adsorbates and the Cu surfaces were measured to provide information about the force needed to break such bonds.

3 Results and Discussion

3.1 Geometry Optimization

3.1.1 Copper Surface

Different generalized gradient approximations (GGA) such as the Wu and Cohen (WC) functional, the PBEsol functional, the Becke Lee Yang Paar (BLYP) functional, the Revised Perdew Burke Ernzerhof (RPBE) functional and

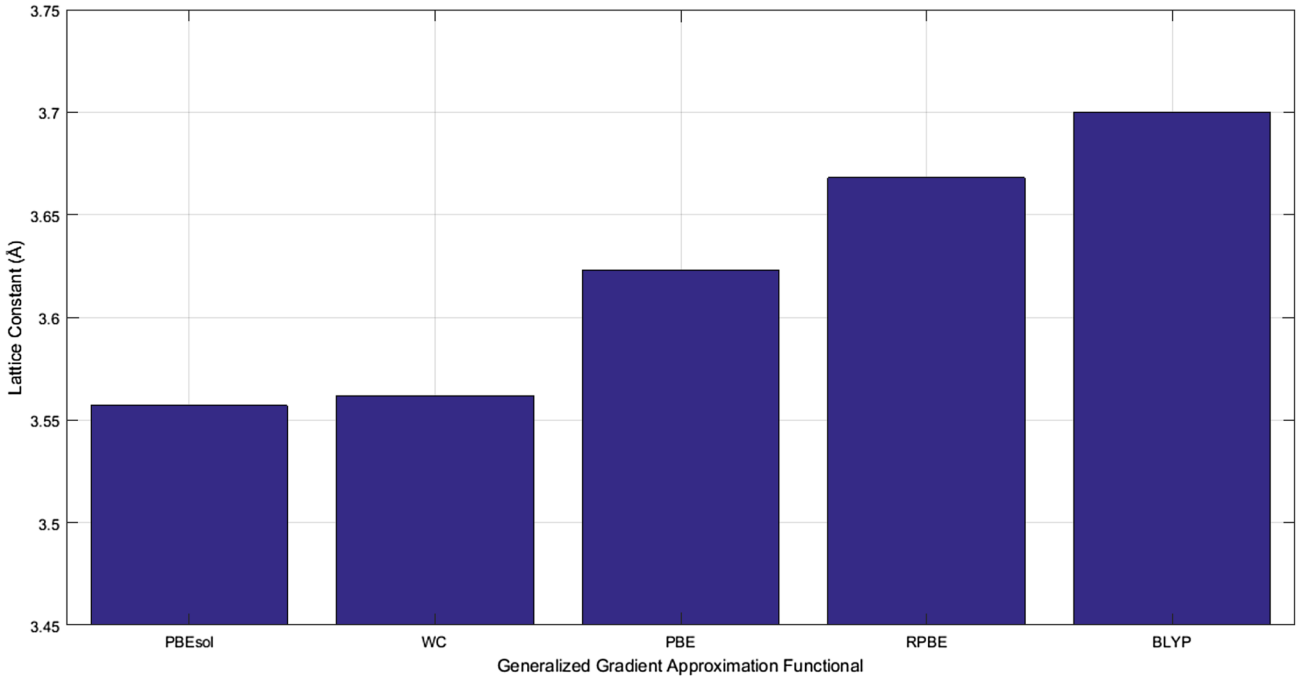

Fig. 3 The lattice constant versus the GGA functional for the Cu bulk

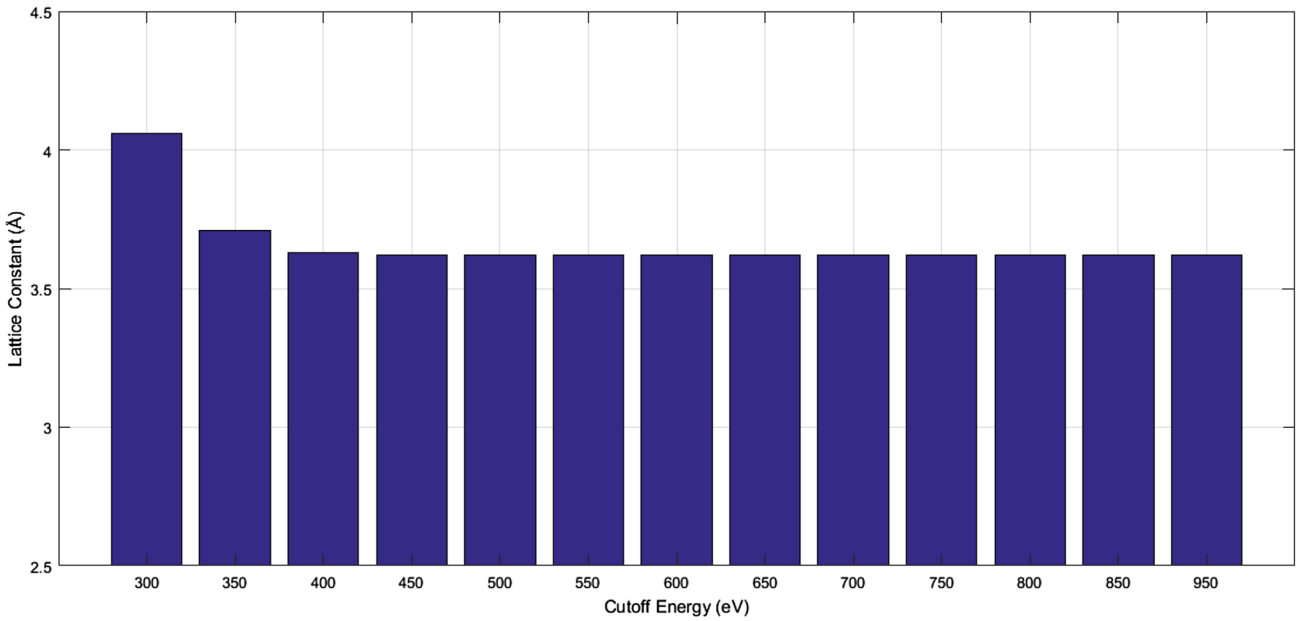

Fig. 4 Lattice constant versus the cutoff energy of the cu bulk

the Perdew–Burke–Ernzerhof (PBE) functional were investigated [24, 29]. By comparing the lattice constant results of the investigated functionals to the experimental lattice constant, the difference in lattice constant was found to be in the range of 0.8% to 8.5%. The GGA PBE exchange-correlation functional [35, 36] was found to produce a lattice constant of 3.623 Å as shown in Fig. 3 which is a difference of 0.8% as compared to the experimental lattice constant of 3.615 Å. The low percentage difference of 0.8% shows that our results are close to the experimental results in references

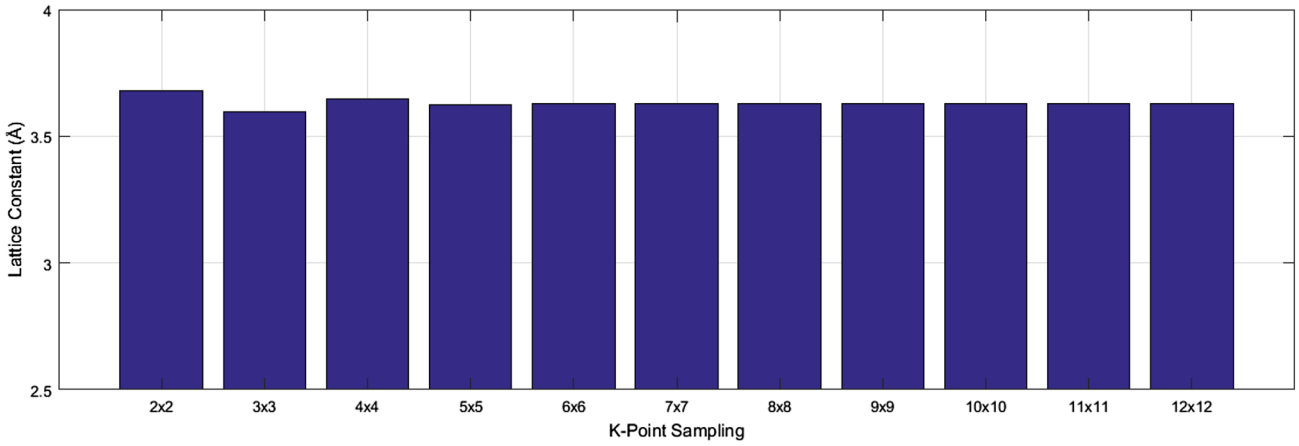

Fig. 5 The lattice constant versus the k-point sampling which showed no change after the 5 × 5 k-point sampling

Table 1 The new optimization energy and lattice constant after the TS correction was applied to the Cu bulk and Cu surfaces

Structure	Energy (eV)	Energy after correction (eV)	Lattice constant (Å)	Lattice constant after correction (Å)	Lattice constant deviation(%)
Cu bulk	− 1681.0	− 1681.6	3.62	3.54	2.2
Cu(100)	− 10084	− 10087	2.52	2.45	2.8
Cu(101)	− 10084	− 10084	2.57	2.53	1.6
Cu(110)	− 10084	− 10086	3.44	3.25	5.5
Cu(111)	− 5041.8	− 5042.9	2.59	2.56	1.2

Table 2 Quantum chemical parameters for DBDS and Cu_2S

Quantum chemical parameter	DBDS	Cu_2S
E_{HOMO} (eV)	− 5.29	− 4.44
E_{LUMO} (eV)	− 1.56	− 3.01
ΔE_{gap}	− 3.73	− 1.43
μ	− 3.43	− 3.72
η	1.87	0.714
δ	0.536	1.40
χ	3.43	3.72

[16, 31] which improves the quality of our research. Our results agree with experimental results in the literature as the PBE exchange-correlation energy functional is commonly used when computing the reactions of molecules with metal surfaces [30, 36–38].

The convergence test results shown in Fig. 4 indicate that the cutoff energy converges to 450 eV when the cutoff energy between 300 to 900 eV was investigated. The k-point sampling results shown in Fig. 5 indicate that the 5 × 5 k-point is the best choice to produce the experimental lattice constant and has minimal difference after the 5 × 5 k-point sampling. The GGA PBE functional with a cutoff energy of 450 eV and k-point of 5 × 5 was therefore used throughout the optimization processes in this study.

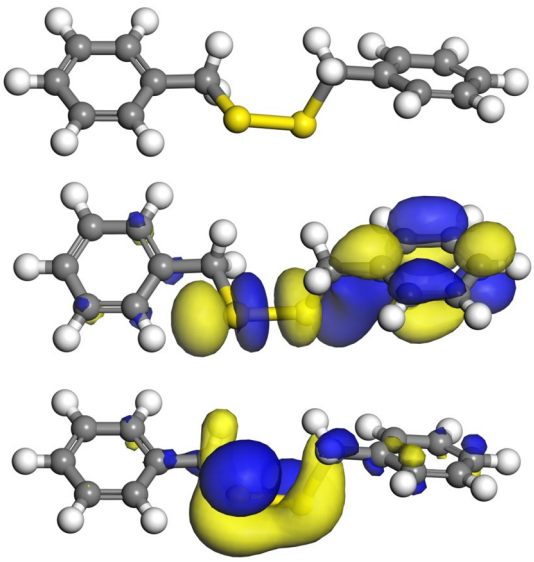

Fig. 6 The optimized DBDS structure, with LUMO and HOMO isosurface respectively. The grey atoms are the carbon atoms while the yellow atoms are the sulphur atoms (Color figure online)

A common disadvantage of using GGA functionals is the lack of representation of the weak forces and the long range interactions forces. To avoid the incorrect influence of the weak forces and long range interaction forces the

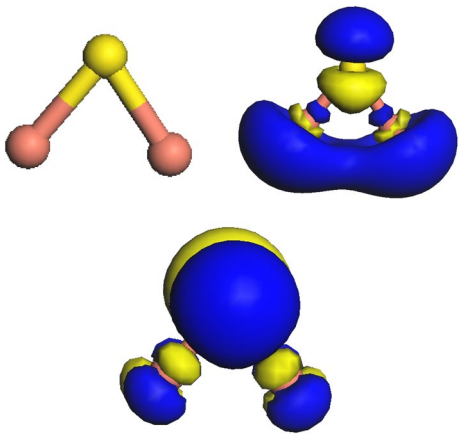

Fig. 7 The optimized Cu_2S structure, with LUMO and HOMO isosurface respectively. The yellow atoms are the sulphur atoms and the brown atoms are the Cu atoms (Color figure online)

Tkatchenko–Scheffler (TS) correction scheme was applied to both the Cu bulk and Cu surfaces [30, 39, 40]. This resulted in changes to the optimizing energy and the lattice parameters as shown in Table 1. However, the energy of the systems remained close to the initial energy before correction while it was observed that the lattice constant changed. An average lattice constant deviation was calculated as 2.7%. The Cu–Cu bond length for surfaces Cu(100), Cu(101), Cu(110) and Cu(111) was computed as 2.499 Å which is close to the value determined in other work [38].

3.1.2 DBDS and Cu_2S

The DBDS and Cu_2S were successfully geometrically optimized using the Dmol^3 module and produced quantum chemical parameters as given in Table 2. The optimized DBDS with its HOMO and LUMO are shown in Fig. 6 while the Cu_2S optimized structure with its HOMO and LUMO are shown in Fig. 7.

The $E_{HOMO}$and E_{LUMO} for the DBDS molecule were found to be − 5.29 eV and − 4.44 eV respectively. The LUMO are evident near both the aromatic methane ring and sulphur atoms while the HOMO are found mainly around the sulphur atoms for the DBDS molecule. The Cu_2S had an E_{HOMO} of − 5.39 eV and an E_{LUMO} of − 1.56 eV. The HOMO in the Cu_2S can also be seen localized around the sulphur atoms while the LUMO is evident around the Cu atoms. When comparing the two adsorbates, the higher E_{HOMO} and lower E_{LUMO} are evident for the Cu_2S which indicates a greater binding ability to the surface. The smaller energy gap of DBDS as compared to Cu_2S indicates that the DBDS is more stable than the Cu_2S and has a smaller probability to donate or accept electrons [41]. The stability of the DBDS adsorbate as compared to the Cu_2S adsorbate is also proven by the higher chemical hardness of 1.87 eV. The lower chemical hardness of Cu_2S indicates the adsorbate is more likely to be deformed than the DBDS adsorbate [22].

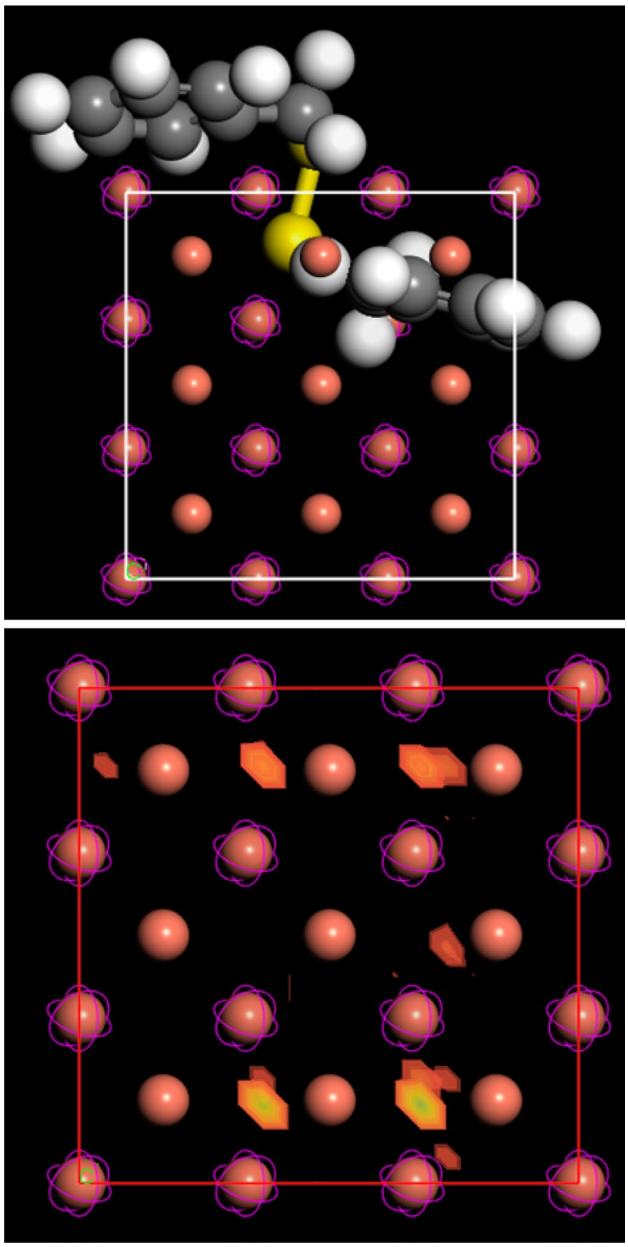

Fig. 8 The lowest energy configuration and density of adsorption sites of DBDS on the Cu(100) surface respectively

3.2 Adsorption Energies

3.2.1 Cu(100) Surfaces

The lowest energy configurations together with its density of adsorption states for the DBDS and Cu_2S molecule on Cu(100) is shown in Figs. 8 and 9 respectively.

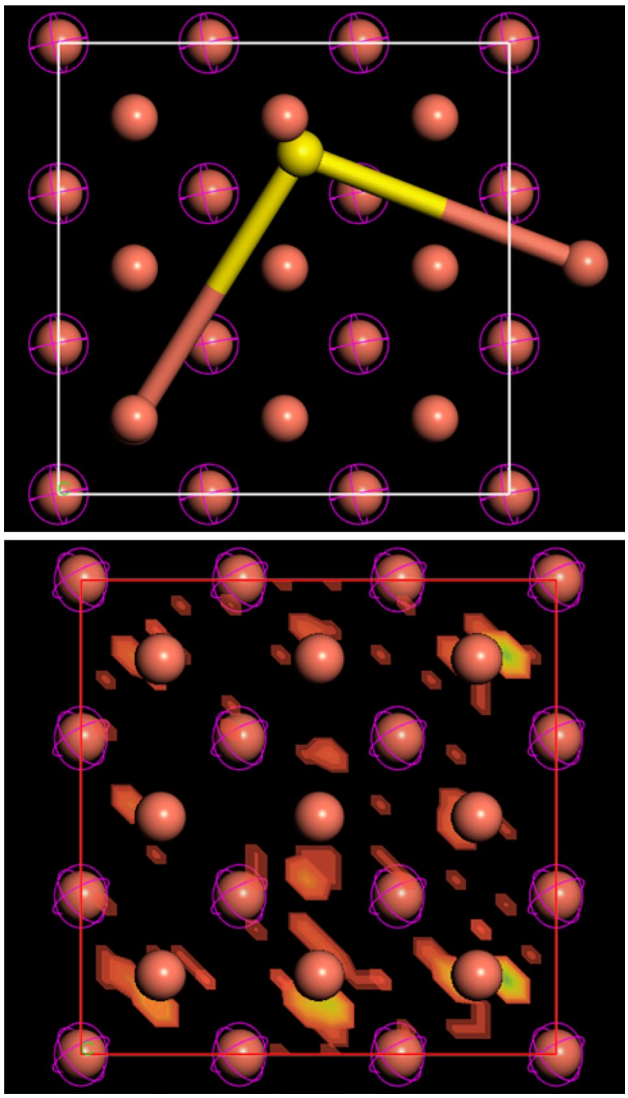

Fig. 9 The lowest energy configuration and density of adsorption sites of Cu_2S on the Cu(100) surface respectively

The adsorption, rigid adsorption and deformation energies for the DBDS and Cu_2S on Cu(100) surfaces are given in Table 3. The Monte Carlo simulation computed only 4 lowest energy configurations for DBDS. The lowest energy configuration produced energies of − 3.925 eV, − 3.197 eV and − 0.7181 eV for the adsorption, rigid adsorption and deformation energies respectively. The Cu_2S was found to have an adsorption, rigid adsorption and deformation energies of − 12.93 eV, − 2.920 eV, − 10.01 eV respectively out of 9 configurations investigated when adsorbed onto the Cu(100) surface. The density of adsorption is illustrated within the Cu lattice in Figs. 8 and 9 and shows a small amount of sites. The Hollow and Top sites were found to be the most likely sites of interaction for DBDS and Cu_2S respectively.

3.2.2 Cu(101) Surfaces

MC simulations computed 9 lowest energy configurations for the DBDS with the Cu(101) surface and produced 11 lowest energy configurations for the interaction of Cu_2S and the Cu(101) surface. The lowest energy configuration and density of sites are shown in Figs. 10 and 11 for the DBDS and Cu_2S respectively. The lowest adsorption energies for DBDS and Cu_2S were found to be − 3.780 eV and − 13.20 eV respectively.The adsorption energy along with the rigid adsorption energy and deformation energy of the DBDS and Cu_2S on Cu(101) surfaces are given in Table 4. The density of adsorption illustrates the most likely adsorption sites to be Hollow sites for both the DBDS and Cu_2S and are a larger set of sites as compared to the Cu(100) surface.

Table 3 The adsorption, rigid adsorption and deformation energies for the DBDS and Cu_2S on Cu(100) surfaces

Cu(100)	DBDS			Cu_2S		
Structure number	Adsorption energy (eV)	Rigid adsorption energy (eV)	Deformation energy (eV)	Adsorption energy (eV)	Rigid adsorption energy (eV)	Deformation energy (eV)
1	− 3.925	− 3.197	− 0.7281	− 12.93	− 2.920	− 10.01
2	− 3.854	− 3.165	− 0.6891	− 12.90	− 2.870	− 10.03
3	− 3.786	− 3.317	− 0.4695	− 12.84	− 2.789	− 10.05
4	− 3.505	− 2.927	− 0.5771	− 12.83	− 2.809	− 10.02
5	–	–	–	− 12.77	− 2.745	− 10.03
6	–	–	–	− 12.75	− 2.723	− 10.03
7	–	–	–	− 12.73	− 2.702	− 10.03
8	–	–	–	− 12.72	− 2.692	− 10.03
9	–	–	–	− 12.70	− 2.684	− 10.02

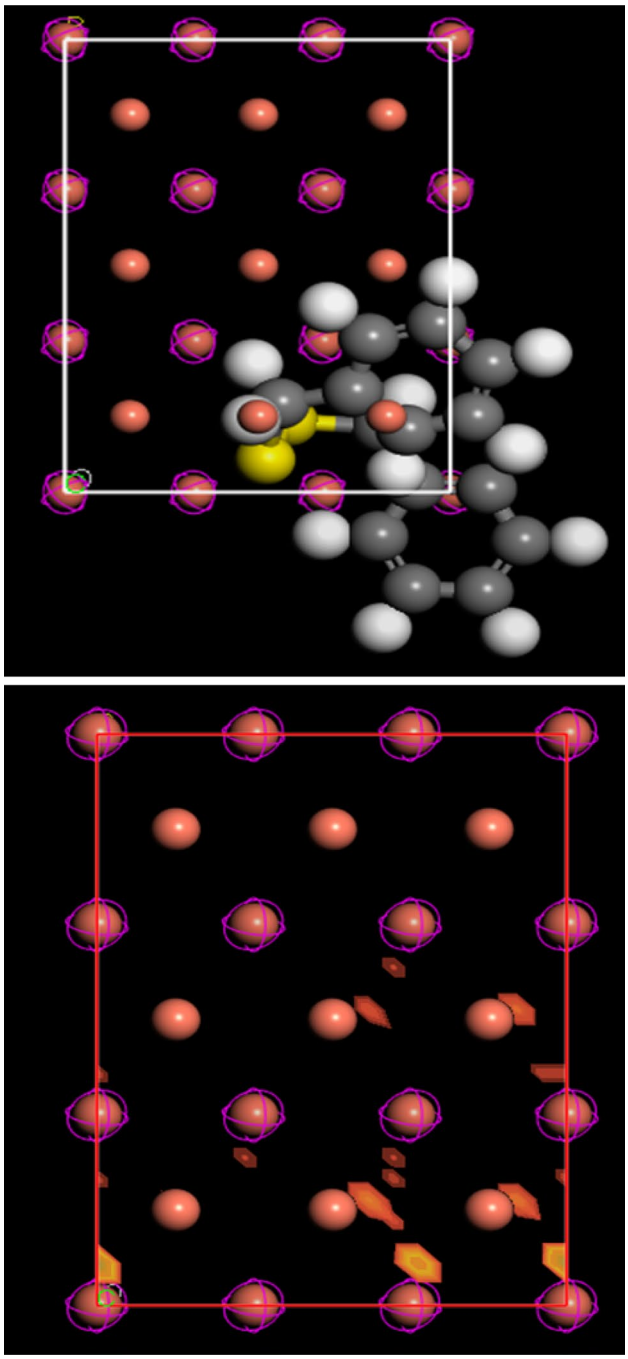

Fig. 10 The lowest energy configuration and density of adsorption sites of DBDS on the Cu(101) surface

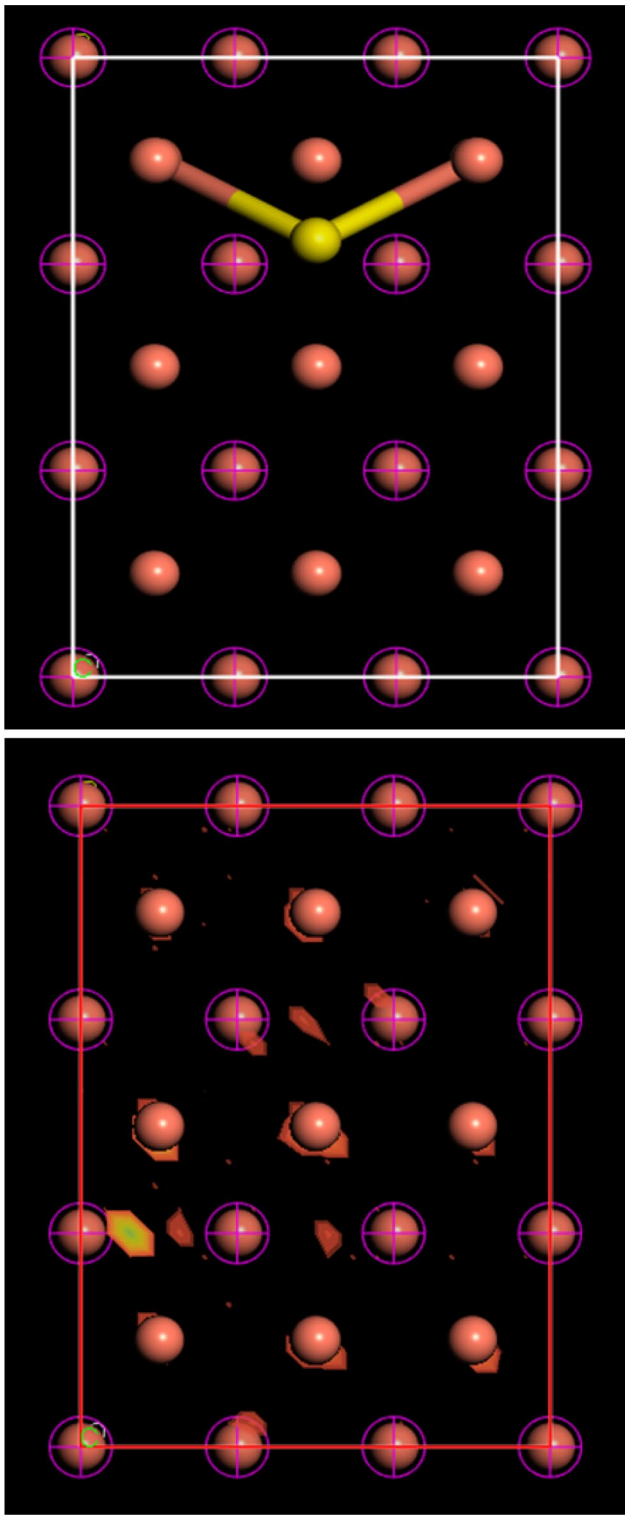

Fig. 11 The lowest energy configuration and density of adsorption sites of Cu_2S on the Cu(101) surface

Table 4 The adsorption, rigid adsorption and deformation energies for the DBDS and Cu_2S on Cu(101) surfaces

Cu(101)	DBDS			Cu_2S		
Structure number	Adsorption energy (eV)	Rigid adsorption energy (eV)	Deformation energy (eV)	Adsorption energy (eV)	Rigid adsorption energy (eV)	Deformation energy (eV)
1	− 3.780	− 3.038	− 0.742	− 13.20	− 3.173	− 10.03
2	− 3.760	− 3.019	− 0.741	− 13.19	− 3.164	− 10.02
3	− 3.718	− 2.976	− 0.741	− 13.16	− 3.139	− 10.02
4	− 3.611	− 3.016	− 0.596	− 13.16	− 3.119	− 10.04
5	− 3.539	− 2.904	− 0.635	− 13.13	− 3.108	− 10.02
6	− 3.511	− 2.944	− 0.568	− 13.11	− 3.099	− 10.01
7	− 3.502	− 2.795	− 0.706	− 13.10	− 3.089	− 10.01
8	− 3.474	− 2.908	− 0.567	− 13.09	− 3.071	− 10.02
9	− 3.440	− 2.937	− 0.504	− 13.08	− 3.072	− 10.01
10	–	–	–	− 13.04	− 3.011	− 10.03
11	–	–	–	− 12.98	− 3.022	− 9.961

3.2.3 Cu(110) Surfaces

Figures 12 and 13 show the lowest energy configuration and density of adsorption sites for DBDS and Cu_2S respectively. The adsorption energies for DBDS and Cu_2S on Cu(110) surfaces were found to be − 3.722 eV and − 13.20 eV respectively and are given in Table 5. The rigid adsorption energy and deformation energy of the DBDS and Cu_2S on Cu(110) surfaces are also provided. The interaction of DBDS with the Cu(110) surface produced 11 lowest energy configurations while the interaction of Cu_2S produced 10 lowest energy configurations. By analyzing the density of adsorption sites illustrations in Figs. 12 and 13 for both the DBDS and Cu_2S, it is evident that the Top sites is the most likely site for interaction.

3.2.4 Cu(111) Surfaces

MC simulations computed 3 and 9 lowest energy configurations for the adsorption of DBDS and Cu_2S on the Cu(111) surface respectively. The lowest energy configurations with their corresponding density of sites are shown in Figs. 14 and 15. The lowest adsorption energies for DBDS and Cu_2S were found to be − 4.254 eV and − 12.78 eV respectively. All energy values for adsorption energy along with the rigid adsorption energy and deformation energy are listed in Table 6. The density of adsorption sites in Figs. 14 and 15 illustrates both DBDS and Cu_2S prefer interacting with the Hollow sites.

All adsorption energies in this paper were found to be negative indicating the reaction is spontaneous and energy is released into the system. The behaviour agrees with experimental work that shows that the corrosive sulphur reaction is spontaneous [3] . Adsorption energies were found to be greater than 0.8eV which indicates that the reactions are all chemisorption reactions [36]. The order of reactivity on the surface was found to be Cu(111) > Cu(100) > Cu(101) > Cu(110) for DBDS. It should be noted that the adsorption on Cu(110) and Cu(101) surfaces produced similar energies that differ by 0.43% for the Cu_2S interacting with the Cu surface. The order of reactivity of the Cu_2S is therefore found as Cu(110) > Cu(101) > Cu(100) > Cu(111). The smaller the adsorption energy the more likely the molecule would be adsorbed as compared to a molecule whose adsorption energy is higher [21]. The adsorbate with the lowest

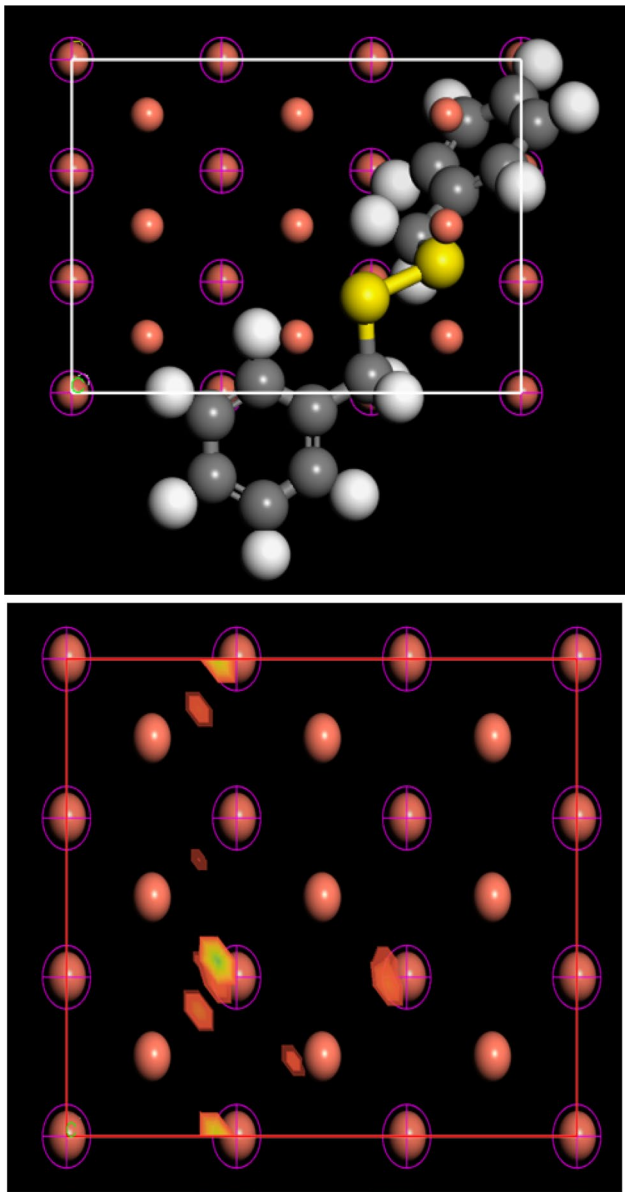

Fig. 12 The lowest energy configuration and density of adsorption sites of DBDS on the Cu(110) surface

adsorption energy is Cu_2S which shows it is more reactive. This agrees with experimental work that Cu_2S interacts with the surface to cause the corrosion of the Cu windings [1–4].

3.3 Bond Lengths

DBDS contains two S molecules and Cu_2S contains one S molecule. The average bond lengths of each S to the nearest Cu surface atom for DBDS and Cu_2S are calculated in Table 7. The average values are 4.845 Å, 5.037 Å and 3.313 Å respectively. The lower bond lengths indicate a higher bond energy which displays the strong bonding nature of the corrosive sulphur and aids in introducing remedial procedures [26]. In this research the Cu_2S was found to have a stronger bonding energy which agrees with experimental work describing the corrosion mechanism of Cu_2S [1–4].

4 Conclusion

The adsorption of two S-containing molecules namely DBDS and Cu_2S on different Cu surfaces were investigated. The Cu bulk, Cu surfaces, DBDS and Cu_2S were all successfully geometrically optimized. The DFT parameters used for the geometry optimization were investigated and found to be the GGA PBE functional with a 5×5 k-point sampling and 450eV cutoff energy. Quantum chemical parameter comparisons were performed on Cu_2S and DBDS. The molecular orbital energy results indicate that Cu_2S is less stable than the DBDS. It was also identified that Cu_2S has a greater binding ability and from the chemical hardness investigation, Cu_2S was found to be more reactive than DBDS.

Monte Carlo simulations were used to compute the adsorption energies, rigid adsorption energies and deformation energies. The lowest adsorption energies for DBDS were found to be − 3.925 eV, − 3.780 eV, − 3.722 eV and − 4.254 eV for the Cu(100), Cu(101), Cu(110) and the Cu(111) surfaces respectively. The lowest adsorption energies for Cu_2S were found to be − 12.93 eV, − 13.20 eV, − 13.20 eV and − 12.79 eV for Cu(100), Cu(101), Cu(110) and the Cu(111) surfaces respectively. The adsorption energies were all identified as spontaneous reactions and are part of a chemisorption process. The Cu_2S molecule was found to be the most reactive corrosive sulphur since the adsorption energy was the lowest. The order of reactivity of the DBDS on the surfaces were found to be Cu(111) > Cu(100) > Cu(101) >Cu(110) while the order of reactivity of the Cu_2S on the Cu surfaces were found to be Cu(110) > Cu(101)>Cu(100) > Cu(111). Our results show

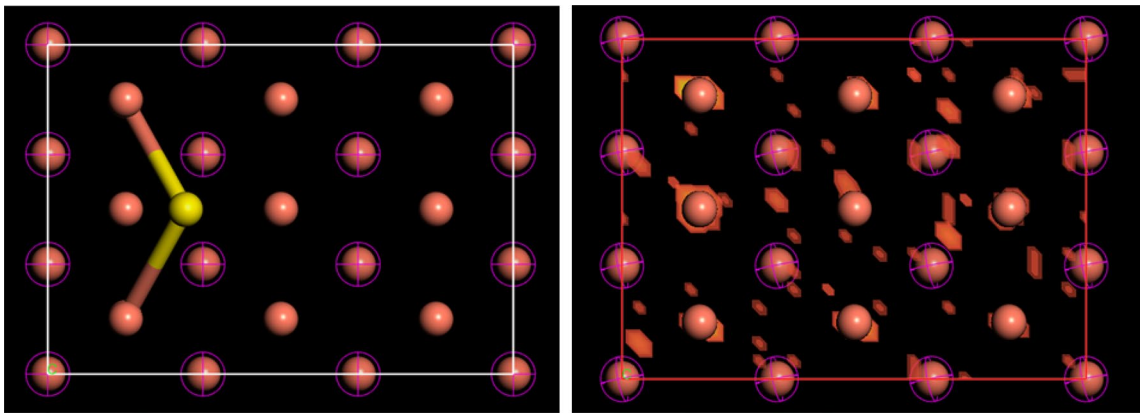

Fig. 13 The lowest energy configuration and density of adsorption sites of Cu_2S on the Cu(110) surface

Table 5 The adsorption, rigid adsorption and deformation energies for the DBDS and Cu_2S on Cu(110) surfaces

Cu(110)	DBDS			Cu_2S		
Structure number	Adsorption energy (eV)	Rigid adsorption energy (eV)	Deformation energy (eV)	Adsorption energy (eV)	Rigid adsorption energy (eV)	Deformation energy (eV)
1	− 3.722	− 3.061	− 0.660	− 13.20	− 3.173	− 10.03
2	− 3.676	− 3.115	− 0.561	− 13.19	− 3.164	− 10.02
3	− 3.638	− 3.116	− 0.522	− 13.16	− 3.119	− 10.04
4	− 3.558	− 3.133	− 0.425	− 13.13	− 3.108	− 10.02
5	− 3.497	− 3.017	− 0.479	− 13.11	− 3.099	− 10.02
6	− 3.445	− 2.829	− 0.616	− 13.10	− 3.089	− 10.02
7	− 3.392	− 2.823	− 0.569	− 13.09	− 3.071	− 10.02
8	− 3.369	− 2.712	− 0.657	− 13.03	− 3.004	− 10.03
9	− 3.345	− 2.799	− 0.546	− 13.02	− 3.000	− 10.02
10	− 3.335	− 2.934	− 0.401	− 12.98	− 3.022	− 9.962
11	− 3.308	− 2.625	− 0.683	–	–	–

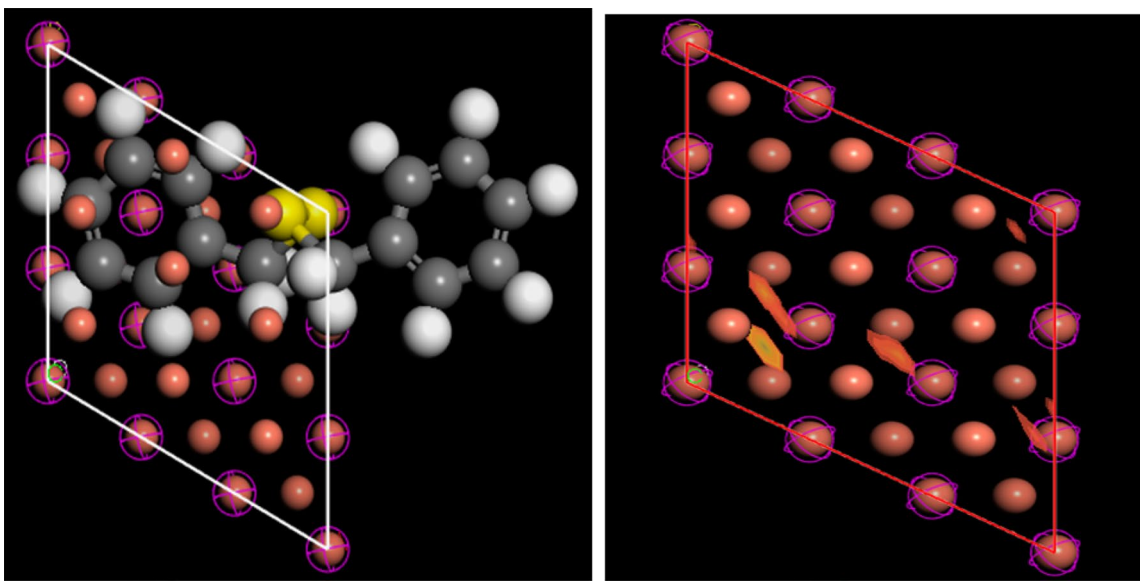

Fig. 14 The lowest energy configuration and density of adsorption sites of DBDS on the Cu(111) surface

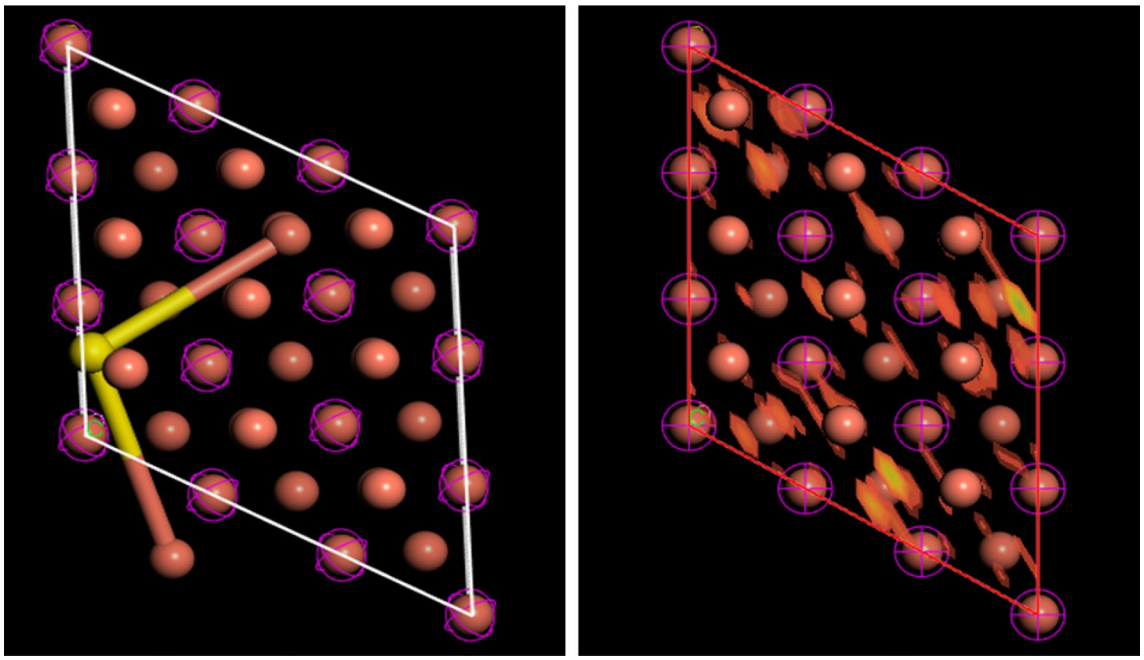

Fig. 15 The lowest energy configuration and density of adsorption sites of Cu_2S on the Cu(111) surface

Table 6 The adsorption, rigid adsorption and deformation energies for the DBDS and Cu_2S on Cu(111) surfaces

Cu(111)	DBDS			Cu_2S		
Structure number	Adsorption energy (eV)	Rigid adsorption energy (eV)	Deformation energy (eV)	Adsorption energy (eV)	Rigid adsorption energy (eV)	Deformation energy (eV)
1	− 4.254	− 3.623	− 0.631	− 12.78	− 2.744	− 10.04
2	− 4.078	− 3.436	− 0.642	− 12.76	− 2.707	− 10,05
3	− 3.953	− 3.398	− 0.555	− 12.73	− 2.698	− 10.03
4	–	–	–	− 12.72	− 2.688	− 10.03
5	–	–	–	− 12.69	− 2.636	− 10.05
6	–	–	–	− 12.57	− 2.542	− 10.03
7	–	–	–	− 12.56	− 2.527	− 10.04
8	–	–	–	− 12.55	− 2.517	− 10.03
9	–	–	–	− 12.50	− 2.485	− 10.01

Table 7 The lowest bond length of the sulphur atom of DBDS and Cu_2S to the nearest Cu surface atom

Surface	DBDS sulphur 1 bond length (Å)	DBDS sulphur 2 bond length (Å)	Cu_2S Sulphur bond length (Å)
Cu(100)	3.374	3.160	3.387
Cu(101)	5.020	3.533	3.333
Cu(110)	6.913	7.399	3.336
Cu(111)	4.071	6.054	3.195
Average bond length	4.845	5.037	3.313

that the interaction of DBDS with the Cu(111) surface and the interaction of Cu_2S with the Cu(110) surface are the most reactive interactions and therefore can be considered to play the major part in the corrosion of transformers. By isolating the Cu surface plane that is mainly involved in corrosion, a passivator can be designed and introduced into the transformer oil in order to reduce the reactivity and increase the adsorption energy such that the DBDS and Cu_2S would not interact with Cu. Future work would entail computationally investigating passivators and films on Cu surfaces, which would reduce the time spent in

understanding the corrosion of transformers using laboratory investigations and likely contribute to the improvement of the lifetime of the power transformers. The bond length investigation between Cu_2S and DBDS indicates that the Cu_2S is more reactive as compared to DBDS. The MC investigation of DBDS obtained in this paper agreed with similar energies determined in theoretical work that investigated the DFT of DBDS [7].

This paper identified the reactivity of the Cu_2S and DBDS in the corrosion mechanism equation by comparing the individual reactivity of the Cu_2S and DBDS with the Cu surface. Our research has identified the Cu_2S to be more reactive than the DBDS which indicates the severity of the corrosion in transformers. The theoretical results in this paper agrees with experimental results which identify that Cu_2S is the reactive species directly involved in the corrosion mechanisms [1–4]. The reactivity of the different corrosive sulphurs brings a better understanding of the corrosion occurring in transformers and allow further remedial procedures to be implemented in the future.

Acknowledgements The authors acknowledge the South African National Research Foundation (NRF) and the Eskom Tertiary Education Support Programme (TESP) for financial support. The authors also acknowledge the Centre for High Performance Computing (CHPC), South Africa, for providing computational resources to this research project.

Funding Funding was provided by the Centre for High Performance Computing (CHPC) South Africa, South African National Research Foundation (Grant No. 83849) and Eskom Tertiary Education Support Programme (TESP).

Compliance with Ethical Standards

Conflict of interest On behalf of all authors, the corresponding author states that there is no conflict of interest.

References

1. Scatiggio F, Tumiatti V, Maina R, Tumiatti M, Pompili M, Bartnikas R (2009) Corrosive sulfur induced failures in oil-filled electrical power transformers and shunt reactors. IEEE Trans Power Deliv 24:1240–1248
2. Toyama S, Tanimura J, Yamada N, Nagao E, Amimoto T (2009) Highly sensitive detection method of dibenzyl disulfide and the elucidation of the mechanism. IEEE Trans Dielectr Electr Insul 16:509–515
3. Maina R, Tumiatti V, Pompili M, Bartnikas R (2009) Corrosive sulfur effects in transformer oils and remedial procedures. IEEE Trans Dielectr Electr Insul 16:1655–1663
4. Oweimreen GA, Jaber AM, Abulkibash AM, Mehanna NA (2012) The depletion of dibenzyl disulfide from a mineral transformer insulating oil. IEEE Trans Dielectr Electr Insul 19:1962–1970
5. Facciotti M, Amaro PS, Holt AF, Brown RC, Lewin PL, Pilgrim JA, Wilson G, Jarman PN (2014) Contact-based corrosion mechanism leading to copper sulphide deposition on insulating paper used in oil-immersed electrical power equipment. Corros Sci 84:172–179
6. Verma C, Haque J, Quraishi MA, Ebenso EE (2019) Aqueous phase environmental friendly organic corrosion inhibitors derived from one step multicomponent reactions: a review. J Mol Liq 275:18–40
7. Saavedra-Torres M, Tielens F, Santos JC (2016) Dibenzyl disulfide adsorption on Cu(111) surface: a DFT study. Theor Chem Acc 135(1):7
8. Samarasinghe WMSC, Martin D, Ma H, Saha TK (2017) A review on influencing factors of sulphur corrosion and metal passivation in power transformers. IEEE AUPEC 1-5
9. Cui H, Zhang X, Zhang G, Tang J (2019) Pd-doped MoS_2 monolayer: a promising candidate for DGA in transformer oil based on DFT method. Appl Surf Sci 470:1035–1042
10. Cui H, Chen D, Zhang Y, Zhang X (2019) Dissolved gas analysis in transformer oil using Pd catalyst decorated $MoSe_2$monolayer: a first-principles theory. SM&T 20:00094
11. Cui H, Jia P, Peng X, Li P (2020) Adsorption and sensing of CO and C_2H_2 by S-defected SnS_2 monolayer for DGA in transformer oil: a DFT study. Mater Chem Phys 249:123006
12. Lee RW, Pan ZY, Hou M (1996) Atomistic simulation of copper cluster deposition on copper. Nucl Instrum Methods Phys Res B 115:536–539
13. Pang XY, Xue LQ, Wang GC (2007) Adsorption of atoms on Cu surfaces: a density functional theory study. Langmuir 23:4910–4917
14. Wahlström E, Ekvall I, Olin H, Lindgren SÅ, Walldén L (1999) Observation of ordered structures for S/Cu(111) at low temperature and coverage. Phys Rev B 60:10699
15. Feibelman PJ (2000) Formation and diffusion of S-decorated Cu clusters on Cu(111). Phys Rev Lett 85:606
16. Alfonso DR, Cugini AV, Sholl DS (2003) Density functional theory studies of sulfur binding on Pd, Cu and Ag and their alloys. Surf Sci 546:12–26
17. Seema P, Behler J, Marx D (2013) Adsorption of methanethiolate and atomic sulfur at the Cu(111) surface: a computational study. J Phys Chem C 117:337–348
18. Soon A, Todorova M, Delley B, Stampfl C (2007) Thermodynamic stability and structure of copper oxide surfaces: a first-principles investigation. Phys Rev B 75:125420
19. Prince NP, Seymour DL, Woodruff DP, Jones RG, Walter W (1989) The structure of mercaptide on Cu (111): a case of molecular adsorbate-induced substrate reconstruction. Surf Sci 215:566–576
20. Ferral A, Patrito EM, Paredes-Olivera P (2006) Structure and bonding of alkanethiols on Cu (111) and Cu (100). J Phys Chem B 110:17050–17062
21. Obot IB, Haruna K, Saleh TA (2019) Atomistic simulation: a unique and powerful computational tool for corrosion inhibition research. Arab J Sci Eng 44:1–32
22. Obot IB, Kaya S, Kaya C, Tüzün B (2016) Theoretical evaluation of triazine derivatives as steel corrosion inhibitors: DFT and Monte Carlo simulation approaches. Res Chem Intermed 42:4963–4983
23. Obot IB, Kaya S, Kaya C, Tüzün B (2016) Density Functional Theory (DFT) modeling and Monte Carlo simulation assessment of inhibition performance of some carbohydrazide Schiff bases for steel corrosion. Physica E 80:82–90
24. Accelrys Software Inc (2011) Accelrys: Materials Studio Release Notes, San Diego
25. Hohenberg P, Kohn W (1964) Inhomogeneous electron gas. Phys Rev 136:B864
26. Square LC, Arendse CJ, Muller TF (2017) Adsorption of phosphoric acid anions on platinum (111). Adsorption 23:971–81

27. El-Sherik AM (2013) Using molecular dynamics simulations and genetic function approximation to model corrosion inhibition of iron in chloride solutions. Int J Electrochem Sci 8:10022–10043
28. Delley B, Ellis DE, Freeman AJ, Baerends EJ, Post D (1983) Binding energy and electronic structure of small copper particles. Phys Rev B 27:2132
29. Clark SJ, Segall MD, Pickard CJ, Hasnip PJ, Probert MI, Refson K, Payne MC (2005) First principles methods using CASTEP. Z Kristallogr Cryst Mater 220:567–70
30. Cui Z, Zhang X, Chen D, Tian Y (2019) Theoretical study on the interaction between SF6 molecule and BaTiO3 (0 0 1) surface: a DFT study. Appl Surf Sci 483:409–16
31. Straumanis ME, Yu LS (1969) Lattice parameters, densities, expansion coefficients and perfection of structure of Cu and of Cu-In α phase. Acta Crystallogr A 25:676–82
32. Dagdag O, El Harfi A, El Gouri M, Safi Z, Jalgham RT, Wazzan N, Verma C, Ebenso EE, Kumar UP (2019) Anticorrosive properties of Hexa (3-methoxy propan-1, 2-diol) cyclotri-phosphazene compound for carbon steel in 3 NaCl medium gravimetric, electrochemical, DFT and Monte Carlo simulation studies. Heliyon 5:1340
33. Lv TM, Zhu SH, Guo L, Zhang ST (2015) Experimental and theoretical investigation of indole as a corrosion inhibitor for mild steel in sulfuric acid solution. Res Chem Intermed 41:7073–7093
34. Sun H, Jin Z, Yang C, Akkermans RL, Robertson SH, Spenley NA, Miller S, Todd SM (2016) COMPASS II: extended coverage for polymer and drug-like molecule databases. J Mol Model 22:47
35. Perdew JP, Burke K, Ernzerhof M (1996) Generalized gradient approximation made simple. Phys Rev Lett 77(18):3865
36. Li Y, Zhang X, Xiao S, Chen D, Chen Q, Wang D (2018) Theoretical evaluation of the interaction between C5-PFK molecule and Cu (1 1 1). J Fluor Chem 208:48–54
37. Li R, Li H, Xu S, Liu J (2017) Combined quantum chemistry and Monte Carlo simulation of competitive adsorption of O2 and OH on Pt surfaces. Appl Surf Sci 410:593–601
38. Huo E, Liu C, Xu X, Li Q, Dang C (2018) Dissociation mechanisms of HFO-1336mzz (Z) on Cu (1 1 1), Cu (1 1 0) and Cu (1 0 0) surfaces: A density functional theory study. Appl Surf Sci 443:389–400
39. Ma S, Jin Y, Si Y (2019) Adsorption behavior of Pd-doped SnS2 monolayer upon H 2 and C 2 H 2 for dissolved gas analysis in transformer oil. Adsorption 25:1587–94
40. Bučko T, Lebègue S, Hafner J, Angyan JG (2013) Tkatchenko–Scheffler van der Waals correction method with and without self-consistent screening applied to solids. Phys Rev B 87:064110
41. Zarrouk A, Hammouti B, Dafali A, Bouachrine M, Zarrok H, Boukhris S, Al-Deyab SS (2014) A theoretical study on the inhibition efficiencies of some quinoxalines as corrosion inhibitors of copper in nitric acid. J Saudi Chem Soc 18:450–455